1.54 μm wavelength emission of highly Er-doped CaF2 layers grown by molecular-beam epitaxy

E. Daran, R. Legros, A. Muñoz-Yagüe, C. Fontaine, and L. E. Bausá

Citation: Journal of Applied Physics **76**, 270 (1994); doi: 10.1063/1.357140
View online: http://dx.doi.org/10.1063/1.357140
View Table of Contents: http://scitation.aip.org/content/aip/journal/jap/76/1?ver=pdfcov
Published by the AIP Publishing

1.54 μm wavelength emission of highly Er-doped CaF_2 layers grown by molecular-beam epitaxy

E. Daran, R. Legros, A. Muñoz-Yagüe, and C. Fontaine
Laboratoire d'Automatique et d'Analyse des Systèmes du CNRS, 7 Avenue du Colonel Roche, 31077 Toulouse Cedex, France

L. E. Bausá
Departamento de Física de Materiales, C-IV, Universidad Autónoma de Madrid, Cantoblanco, 28049 Madrid, Spain

(Received 23 December 1993; accepted for publication 10 March 1994)

CaF_2:Er layers have been grown by molecular-beam epitaxy on (100)-oriented CaF_2 substrates; the Er concentration ranges from 1% to 50% (mole fraction). The 1.54 μm emission observed under excitation around 800 nm was studied by photoluminescence. Up to 35% Er concentration the integrated emission increases monotonously, quenching appearing for higher doping levels. Photoluminescence results are discussed within the framework of previous studies of Er^{3+} emission in the near-infrared range (830–860 nm) in order to gain insight into the Er centers involved in the 1.54 μm emission.

I. INTRODUCTION

In recent years, rare-earth-doped materials such as thin films have received considerable attention. The aim of the works published was to take advantage of the optical characteristics of the rare-earth ions to be incorporated in miniaturized or integrated optical devices. In particular, Er-doped materials are becoming increasingly popular in view of their application in laser-diode-pumped amplifiers at 1.54 μm wavelength.

The authors first demonstrated that molecular-beam epitaxy (MBE) is a suitable technique for growing Nd-doped CaF_2 monocrystalline layers on CaF_2, GaAs, and Si substrates.[1,2] More recently, they investigated Er^{3+} incorporation in CaF_2 MBE homoepitaxial layers and the effect of the growth conditions, on the basis of spectroscopic characterization by photoluminescence in the 830–860 nm wavelength range associated with the $^4S_{3/2} \rightarrow {}^4I_{13/2}$ transitions for layers doped up to 6 mol % of Er^{3+} ions.[3,4]

In good agreement with the results obtained for bulk material, a spectral complexity could be shown. Two types of single Er^{3+} centers and three aggregate Er^{3+} centers were identified. As to Nd^{3+}-doped MBE CaF_2 layers, the growth technique used has shown its ability to modulate the relative proportion of the different crystalline sites. First, depending on the epitaxial conditions, different types of emission centers can be induced. Second, compared to bulk crystal, for a given Er content, a lower proportion of aggregate centers relative to isolated Er^{3+} sites can be obtained, this effect being reasonably explained by the thermodynamic conditions imposed by MBE.

In this article the infrared emission (IR) of Er^{3+} ions is studied in depth for the first time in such layers. We report the spectroscopic characteristics associated with the $^4I_{13/2} \rightarrow {}^4I_{15/2}$ transition of Er^{3+} ions. Excitation was performed around 800 nm and involved the $^4I_{15/2} \rightarrow {}^4I_{9/2}$ transition of Er^{3+} while the corresponding excitation spectra in this region were given, yielding the wavelengths needed to excite the IR emission using GaAlAs-GaAs laser diodes. In addition, the Er concentration studied has been dramatically enlarged (up to 50%) and the effect of the analysis temperature on the emission of interest is also shown. Due to the multiplicity of levels involved in the $^4I_{13/2} \rightarrow {}^4I_{15/2}$ transition and the variety of Er^{3+} sites with different crystalline symmetries, the centers causing the 1.54 μm emission are difficult to identify for high Er concentrations; however, the nature of the centers involved, useful for further optimization, is discussed on the basis of the results obtained.

II. EXPERIMENT

The CaF_2:Er^{3+} layers studied were grown by MBE using two effusion cells containing CaF_2 and ErF_3, respectively. Prior to the study, flux calibration was carried out from thickness measurements of layers of each type grown on Si substrates at different cell temperatures. Then, the CaF_2 cell was operated at 1210 °C to obtain a growth rate of 0.5 μm/h while the ErF_3 temperature was varied to obtain the desired Er concentration. It was found by Rutherford backscattering (RBS) measurements that the entire ErF_3 flux gives rise to an effective Er incorporation in the crystalline lattice of the growing CaF_2 matrix. The Er molar fraction in the doped layers is calculated from the molar cation ratio: Er/(Er+Ca).

The MBE technique retained offers two advantages: (i) thermodynamic growth conditions are quite different from those imposed for bulk crystal and a more favorable distribution (lower clustering) of doping impurities in the host lattice can be expected; (ii) the use of a rare-earth (RE) trifluoride allows quasi-intrinsic charge compensation due to the excess F^- interstitials available when a trivalent Er cation replaces a divalent Ca cation.

(100)-oriented CaF_2 substrates were used; after being degreased and In soldered on a molybdenum block they were loaded into the ultrahigh-vacuum system. There, the substrates were heated up to 550 °C then to 520 °C, and growth was initiated. The Er-doped layers grown were 2 μm thick.

 0021-8979/94/76(1)/270/4/$6.00

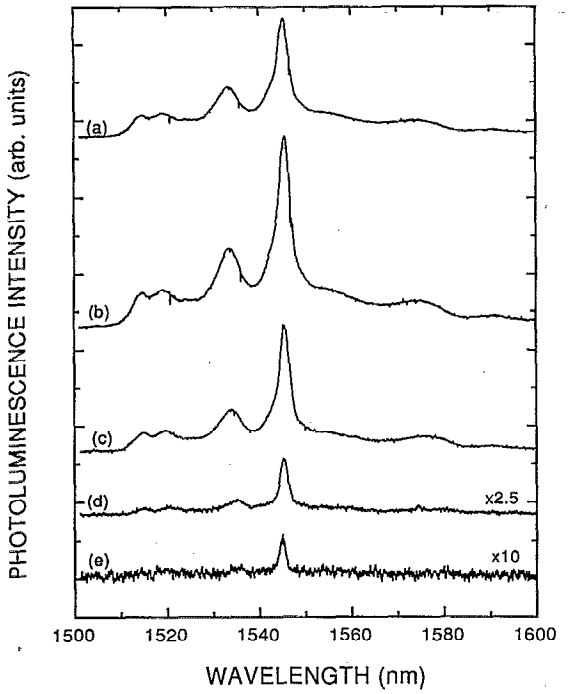

FIG. 1. Er^{3+} luminescence spectra in the $^4I_{13/2} \rightarrow {}^4I_{15/2}$ region at 77 K for CaF_2 layers grown under the same conditions with a different Er^{3+} content: (a) 45.6; (b) 35.4; (c) 23.5; (d) 8.7; (e) 1.8 mol % Er^{3+}.

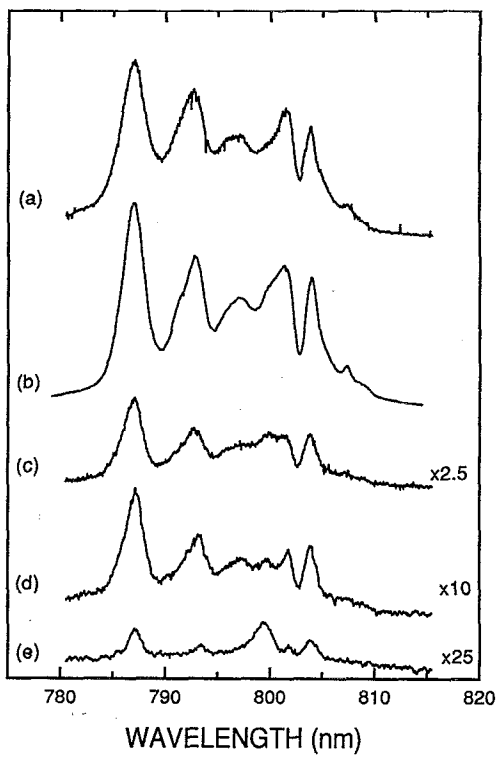

FIG. 2. Excitation spectra of the $^4I_{15/2} \rightarrow {}^4I_{9/2}$ Er^{3+} transition for (a) 45.6; (b) 35.4; (c) 23.5; (d) 8.7; (e) 1.8 mol % Er^{3+} in CaF_2.

A tunable Ti-sapphire laser was used as excitation source for both emission (PL) and excitation (PLE) photoluminescence measurements at 77 K. A $f=1$ m monochromator and a cooled Ge detector followed by a lock-in amplifier were used for detection.

III. RESULTS AND DISCUSSION

A. Spectroscopic analysis of the 1.54 μm emission

Figure 1 shows the emission spectra associated with the $^4I_{13/2} \rightarrow {}^4I_{15/2}$ transition of Er^{3+} obtained at low temperature for a series of layers grown under the same conditions but with different Er concentrations. The excitation was carried out at 786 nm which lies in the $^4I_{15/2} \rightarrow {}^4I_{9/2}$ transition of the free ion. As can be seen, some weak peaks, together with a sharp emission line at 1.54 μm, are detected for the whole Er concentration range. The position of the emission lines and their relative intensity do not show dramatic changes for the concentration range studied.

In order to obtain more data, excitation photoluminescence measurements were also performed on these layers, whose spectra are given in Fig. 2. These were obtained by monitoring the same emission wavelength, 1.54 μm, which corresponds to the maximum intensity of the sharp line in Fig. 1. Clearly, the shape of the excitation spectra, as well as the number of detected peaks, depend on the Er concentration.

It is also worth recalling previous results on samples doped up to 6% Er for the emission corresponding to the $^4S_{3/2} \rightarrow {}^4I_{13/2}$ transitions.[4] The lines observed could be successfully associated with the different Er^{3+} centers already reported for Er-doped CaF_2 bulk crystals:[5] single Er^{3+} centers, C_{3v} and C_{4v}, and aggregate Er^{3+} centers, $D(1a)$, $D(2a)$, and C. When the Er concentration rose these different emission centers in MBE CaF_2 layers evolved as in bulk CaF_2:[6] the signals related to Er^{3+} aggregate centers $D(1a)$ and $D(2a)$ rose monotonously with the Er content, while the other emissions, corresponding to single Er^{3+} and C aggregate centers, decreased. For layers doped with 5 mol %, the $D(2a)$ aggregate center becomes dominant.

When comparing photoluminescence characteristics obtained in the two wavelength ranges, special care has to be taken because excitation and detection in the present study around 1.54 μm are carried out in a manner different from the previous analysis in the 830–860 nm range. Nonetheless, some common features can be noted in the respective emission spectra which correspond to CaF_2 layers with moderate Er contents (<8%). Indeed, a parallelism can be established between the emission related to the $D(2a)$ aggregate center identified in the 800 nm region and the emission at 1.54 μm when considering their variation with Er concentration as can be seen in Fig. 3. This suggests that, at least for moderately doped samples, the line at 1.54 μm would be associated with this type of aggregate centers, which have been associated with a dimerization state of Er^{3+} ions in previous works on Er-doped bulk materials.[7] This is supported by the excitation spectrum of the lowest doped layer [Fig. 2(d)]. It only exhibits five peaks in good agreement with the multiplicity of the $^4I_{9/2}$ excited multiplet which indicates the presence of only one Er^{3+} center in a noncubic symmetry which would thus be the $D(2a)$ center. The $^4I_{9/2}$ stark sublevels for this

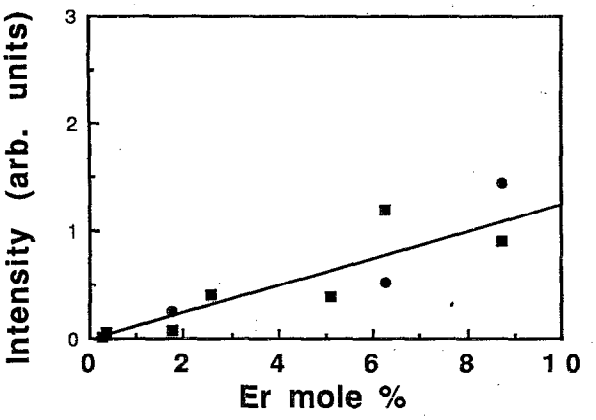

FIG. 3. Intensity emission of a $D(2a)$ site at 845.4 nm (□) and integrated intensity emission in the range (1.5–1.6 μm) (○) as a function of Er^{3+} concentration for (100) CaF_2:Er layers.

aggregate Er^{3+} center obtained directly from this excitation spectrum are given in Table I.

For higher (>8%) Er contents, the excitation spectra (Fig. 2) become more complex as the Er concentration increases. On the one hand, the shape of the spectra progressively changes and, at least, an additional peak is observed. On the other hand, the peak positions are slightly changed toward the higher energies as the Er concentration rises.

With respect to the emission spectra, a shoulder on the main emission peak and an overall broadening can be observed in Fig. 1; these features are more clearly evidenced in Fig. 4 which yields two normalized emission spectra for the CaF_2 layers with 1.8% and 45.5% Er concentrations. This could be an inhomogeneous broadening originating from the presence of a variety of Er ions in a very similar crystal-field position for the higher Er^{3+} concentrations; however, no extra lines on the emission spectra are found, as can be seen in Fig. 1. Similar concentration effects were reported for bulk CaF_2:Er, but they were found to occur at lower Er concentrations[7] than in the present case.

For more data, site-selective excitation experiments were carried out inside the $^4I_{15/2} \rightarrow {}^4I_{9/2}$ transition by tuning the excitation and emission wavelengths. No changes in the PL and PLE spectra could be detected when changing the monitored wavelengths. This shows the different Er^{3+} sites producing broadening of the 1.54 μm to be in very close energy positions with overlapping absorption lines. All these results, related to the high Er concentrations involved, could be accounted for in several ways. For example, it could be said that, in addition to the initial $D(2a)$ center, other emission centers of the same $D(2)$ family are formed due to the Er^{3+} ions proximity. Indeed, they were observed in bulk CaF_2:Er and shown to overlap the $D(2a)$ emission.[8] Further work still has to be carried out for a more precise assignment.

TABLE I. Energy levels of the $^4I_{9/2}$ multiplet of Er^{3+} $D(2a)$ site in units of cm^{-1} observed in layers of CaF_2:Er 1.8 mol % at 77 K.

$D(2a)$ site	12706.5
	12602.4
	12510.9
	12471.9
	12440.9

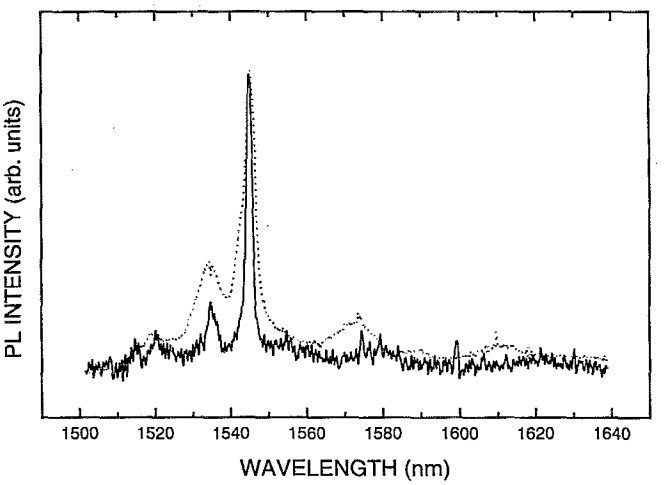

FIG. 4. Photoluminescence spectra of two CaF_2:Er (100) layers in the $^4I_{13/2} \rightarrow {}^4I_{15/2}$ region. Solid line: 6 mol %; dotted line: 45.6 mol %.

B. Concentration and temperature effects on the 1.54 μm emission intensity

A more interesting idea of the effect of Er concentration on the 1.54 μm emission can be inferred from Fig. 5, which shows the 1.54 μm integrated emission variation as a function of Er concentration. The intensity increases monotonously up to an Er concentration of 35%. Then, at higher doping levels, luminescence quenching occurs due to a nonradiative relaxation process. Concentration quenching can be accounted for by energy transfer between close Er^{3+} ions. The presence of Er^{3+} aggregate centers such as the $D(2)$-type centers supports this. On the other hand, an efficient energy-transfer process has been observed in these layers to give rise to an infrared to green up-conversion emission process which will be reported elsewhere. To our knowledge, it

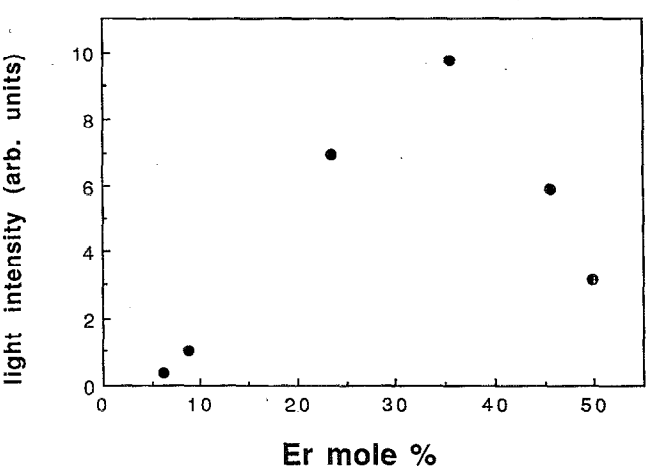

FIG. 5. Integrated light intensity emission in the range (1.5–1.6 μm) as a function of Er^{3+} concentration for (100) CaF_2:Er layers.

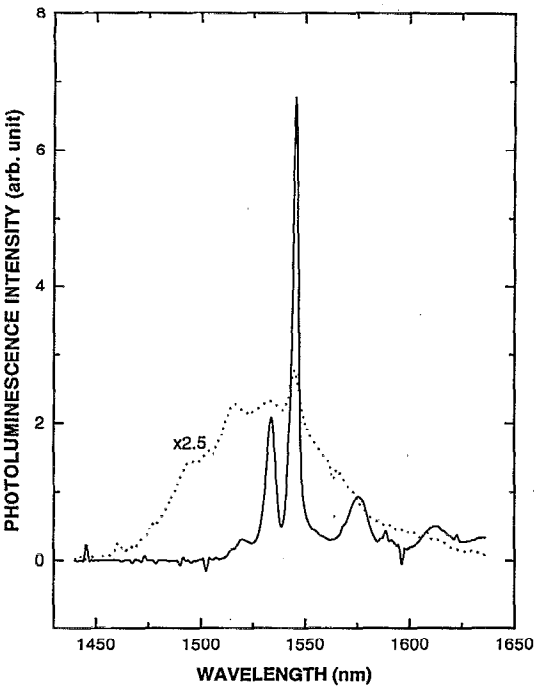

FIG. 6. Photoluminescence spectra of a CaF_2 layer doped 35.4 mol % Er^{3+} at 77 K (solid line) and 300 K (dotted line). Note that the spectrum at 300 K has been increased by 2.5 relative to that at 77 K.

is the highest optimal value reported so far. It was found to be of the order of 5% in bulk CaF_2:Er,[8] and, in that case, the limit in the doping level to preserve crystal quality was given to be 10 mol %.[9] In the present case, reflection high-energy electron-diffraction (RHEED) observations did not evidence any noticeable degradation of the layer crystallinity for the whole Er concentration range. Moreover, no change in the aspect of the grown layers was observed, which remain transparent and of good surface morphology in all cases. This confirms the ability of the MBE technique to grow this type of layer.

The effect of the PL temperature on the 1.54 μm emission was finally investigated. Figure 6 allows us to compare the spectra obtained on the same CaF_2:Er layer at 77 K and 300 K. Care was taken to keep the same analysis conditions. An overall emission broadening and an intensity decrease of the main emission line are observed for the higher temperature. These two effects balance each other and, as a result, the integrated intensity was measured to be the same for both temperatures. This result shows that losses due to a nonradiative recombination are not strong, probably due to the low phonon energy of the fluoride host, and that the use of this emission at room temperature can be envisaged.

IV. CONCLUSIONS

Monocrystalline layers of CaF_2:Er have been grown by MBE with Er concentrations up to 50%, without noticeable degradation of the layer crystallinity. All the layers were shown to exhibit a sharp emission at 1.54 μm at low temperature.

A spectroscopic analysis of this emission line has been performed using photoluminescence excitation in the spectral range 780–810 nm. Together with the previously reported results for emission in the 830–860 nm region, that analysis suggests that the Er^{3+} centers involved in the 1.54 μm emission are complex centers and that they would be the $D(2)$ centers identified in previous works on the near-infrared emissions.

The 1.54 μm emission, although broadened, was observed to keep a nearly constant intensity at room temperature. The integrated luminescence intensity has been found to increase monotonously up to 35% Er, beyond which concentration quenching occurs. These are, to our knowledge, the highest optimal values reported for Er-doped materials and further evidence of the capability of the MBE technique to grow Er-doped fluoride layers emitting at 1.54 μm, which is the standard wavelength in optical telecommunications.

ACKNOWLEDGMENTS

The authors are grateful to G. Lacoste for technical assistance and M. Dupuy and F. Pierre (CENG-Grenoble) for RBS measurements. This work was supported by the ULTIMATECH program of CNRS.

[1] L. E. Bausa and A. Muñoz-Yagüe, Appl. Phys. Lett. **59**, 3511 (1991).
[2] L. E. Bausa, C. Fontaine, E. Daran, and A. Muñoz-Yagüe, J. Appl. Phys. **72**, 499 (1992).
[3] E. Daran, L. E. Bausa, A. Muñoz-Yagüe, and C. Fontaine, Appl. Phys. Lett. **62**, 2616 (1993).
[4] E. Daran, R. Legros, A. Muñoz-Yagüe, and C. Fontaine, J. Appl. Phys. **75**, 2749 (1994).
[5] D. R. Tallant and J. C. Wright, J. Chem. Phys. **63**, 2074 (1975).
[6] D. R. Tallant, D. S. Moore, and J. C. Wright, J. Chem. Phys. **67**, 2897 (1977).
[7] J. B. Fenn, J. C. Wright, and F. K. Fong, J. Chem. Phys. **59**, 5591 (1973).
[8] D. S. Moore and J. C. Wright, J. Chem. Phys. **74**, 1626 (1981).
[9] S. A. Pollack, D. B. Chang, and N. L. Moise, J. Appl. Phys. **60**, 4077 (1986).